

## Combined mean-field and three-body model tested on the $^{26}\text{O}$ nucleus

D. Hove,<sup>1</sup> E. Garrido,<sup>2</sup> P. Sarriguren,<sup>2</sup> D. V. Fedorov,<sup>1</sup> H. O. U. Fynbo,<sup>1</sup> A. S. Jensen,<sup>1</sup> and N. T. Zinner<sup>1</sup>

<sup>1</sup>*Department of Physics and Astronomy, Aarhus University, DK-8000 Aarhus C, Denmark*

<sup>2</sup>*Instituto de Estructura de la Materia, IEM-CSIC, Serrano 123, E-28006 Madrid, Spain*

(Received 14 December 2016; published 1 June 2017)

We combine few- and many-body degrees of freedom in a new computationally efficient model applicable to both bound and continuum states and adaptable to different subfields of physics. We formulate a self-consistent three-body model for a core nucleus surrounded by two valence nucleons, where the core is treated in the mean-field approximation and the same effective Skyrme interaction is used between both core and valence nucleons. We apply the model to  $^{26}\text{O}$ , where we reproduce the known experimental data as well as phenomenological models with more parameters. The decay of the ground state is found to proceed directly into the continuum without effect of the virtual sequential decay through the well-reproduced  $d_{3/2}$  resonance of  $^{25}\text{O}$ .

DOI: [10.1103/PhysRevC.95.061301](https://doi.org/10.1103/PhysRevC.95.061301)

**Introduction.** Self-consistent mean-field calculations efficiently provide accurate average properties for  $N$ -body systems [1–3]. A long list of other methods have been developed in an attempt to treat correlated systems [4–10]. All these methods are first of all aimed at describing bound states. Resonances, their decay, and continuum states in general are often addressed, but only with much more difficulty. The challenges are often referred to as problems in connection with open quantum systems [11]. This concept is defined as quantum systems in interaction with the environment via external fields or, more appropriate in the present context, by coupling to continuum degrees of freedom.

When the number of particles is less than about 15, complete correlated, *ab initio* solutions, fitted to some fundamental, observed properties, can be obtained [12–14]. This limit is gradually being increased, but the complexity increases exponentially with the number of particles, and progress is slow. The solutions are obtained with few-body techniques that are as analytically or numerically accurate as necessary in the context. Thus, all necessary effects from couplings to the continuum can in principle be fully included for light systems. Moderately heavy systems can also be treated using various approximations or simplifications [15]. Generally, these few-body techniques are designed to operate for distances larger than the radii of the fundamental, constituent particles necessarily assumed to be inert. This is in contrast to the many-body methods designed to treat approximately bound or at least quasistable states at small distances.

Few of the existing methods can treat both small-distance structure and large-distance decay properties with even approximately the same level of detail. Generally, the traditional few-body cluster methods assume small-distance boundary conditions at the surface of the constituent particles and provide corresponding large-distance behavior. The many-body methods provide detailed small distance structures and therefore correct boundary conditions for few-body calculations. Those extended *ab initio* models that attempt a detailed treatment of both small- and large-distance aspects, such as the no-core shell model with couplings to continuum [12], do so at the expense of great computational complexity [16,17]. Not only are such models limited to a low number of total particles,

but also two- and in particular three-body cluster structures are very difficult to incorporate.

The ideal model would treat small- and large-distance structures equally well, while also be able to describe cluster configurations for any type of system, light or heavy. The combination of these properties in one model would be extremely useful and of general interest in all subfields of physics. More so, if the combination could be done with less of a computational limitation and thereby more flexibility. Specifically, a number of interdisciplinary topical problems can be better understood microscopically. This applies in particular to the concept of universality in connection with halo formation and decay [18] and the extreme of Efimov physics [19]. Both phenomena appear in nuclei and nuclear astrophysics, as well as in cold atomic and molecular gases.

The purpose of this Rapid Communication is to provide an overall framework for a simple combination of the few- and many-body treatments of relative and intrinsic motion of the constituent particles. We shall use the hyperspherical adiabatic Faddeev expansion method for the few-body part [20] and the mean-field approximation for the many-body part [21]. The applied many-body effective interaction is in this Rapid Communication consistently incorporated in the few-body treatment. As is always the case when expanding the Hilbert space, the interactions must be renormalized for use in the expanded space, which can pose a challenge. Most *ab initio* models focus on the need to establish some fundamental interaction, which is used to derive the more complicated, multiparticle structures. The equally critical Hilbert space is assumed to adjust accordingly. Here, the expansion of the Hilbert space will be treated more explicitly.

The simple implementation we have investigated as illustration of the method requires a spherical mean-field core. We added the valence particles on top of the Fermi surface where the Pauli exclusion from core neutrons is most easily taken into account. This implies that the two-neutron separation energy preferentially should be small since for simplicity we used the free  $NN$  interaction between these two particles. Both conditions can be relaxed by appropriate modifications left for future work.

The practical implementation is crucial to test applicability, accuracy, and efficiency. We choose  $^{26}\text{O}$ , where the nucleons in  $^{24}\text{O}$  core and the additional two neutrons require different treatment [22] and where the traditional methods are inappropriate. The  $^{26}\text{O}$  nucleus is an ideal test case on the neutron dripline with the double magic [23] and spherical  $^{24}\text{O}$  core and the two valence neutrons [24–26]. However, the method is not limited to light nuclei and can be applied to any system where a mean-field calculation can produce a self-consistent solution.

*Theoretical formulation.* We consider an  $A + 2$  nucleon system divided into a core with mass number  $A$  and two valence nucleons. We assume the same two- and three-body interactions,  $V_{ij}$  and  $V_{ijk}$ , acting between all the nucleons in core and valence space. The general Hamiltonian can then be written

$$H = \sum_{i=1}^{A+2} T_i - T_{\text{cm}} + \sum_{i<j}^{A+2} V_{ij} + \sum_{i<j<k}^{A+2} V_{ijk}, \quad (1)$$

where  $T_i$  and  $T_{\text{cm}}$  are the kinetic energy operators for the  $i$ th nucleon and for the total  $A + 2$  system, respectively. We reorganize  $H$  into terms related to core,  $H_c$ , and valence,  $H_v$ , particles, i.e., explicitly

$$H = H_c(\mathbf{r}_1, \dots, \mathbf{r}_A) + H_v(\mathbf{r}_{v_1}, \mathbf{r}_{v_2}), \quad (2)$$

$$H_c = \sum_{i=1}^A T_i - T_{\text{cm}}^{\text{core}} + \sum_{i<j}^A V_{ij} + \sum_{i<j<k}^A V_{ijk}, \quad (3)$$

$$\begin{aligned} H_v = & T_{\text{cm}}^{\text{core}} + T_{A+1} + T_{A+2} - T_{\text{cm}} + V_{A+1,A+2} \\ & + \sum_{i=1}^A (V_{i,A+1} + V_{i,A+2}) + \sum_{i=1}^A V_{i,A+1,A+2} \\ & + \sum_{i<j}^A (V_{i,j,A+1} + V_{i,j,A+2}) \end{aligned} \quad (4)$$

where the spin, isospin, and space coordinates of the  $i$ th core or valence nucleons are  $\mathbf{r}_i$  and  $\mathbf{r}_{v_i}$ , respectively.

The decisive approximation is now the choice of the Hilbert space allowed for the wave function, that is

$$\Psi = \mathcal{A}(\Phi_c(\mathbf{r}_1, \dots, \mathbf{r}_A)\Phi_v(\mathbf{r}_{v_1}, \mathbf{r}_{v_2})), \quad (5)$$

where  $\Phi_c = \det(\{\phi_i\})$  is the Slater determinant, of single-particle wave functions,  $\phi_i$ , for the core nucleons,  $\Phi_v$  is the three-body wave function, and  $\mathcal{A}$  symbolizes antisymmetrization of all nucleons. The form of  $\Psi$  in Eq. (5) clearly exhibits how we combine mean-field treatment of the core and ordinary treatment of the two three-body relative degrees of freedom. The total energy,  $E$ , is a sum of two terms corresponding to core,  $E_c$ , and valence,  $E_v$ , Hamiltonians in Eq. (2), that is

$$E = E_c + E_v = \langle \Psi | H_c | \Psi \rangle + \langle \Psi | H_v | \Psi \rangle. \quad (6)$$

We find the equations for the lowest energy solution by varying the wave functions over the allowed Hilbert space, that is,

$$\frac{\delta E}{\delta \Phi_c^*} = \frac{\delta E}{\delta \Phi_v^*} = 0, \quad (7)$$

where both  $\Phi_c$  and  $\Phi_v$  must be normalized during the variation. The forms of the two resulting equations are

$$H_{\text{HF}}(\Phi_v, \Phi_c)\phi_i = \epsilon_i\phi_i; \quad H_v(\Phi_v, \Phi_c)\Phi_v = E_v\Phi_v, \quad (8)$$

where the effective interactions in both Hartree-Fock single-particle,  $H_{\text{HF}}$ , and three-body,  $H_v$ , Hamiltonians depend on both  $\Phi_c$  and  $\Phi_v$ . The coupled equations in Eqs. (8) must be solved simultaneously, which in practice means iteratively, to determine  $\Phi_c$  and  $\Phi_v$ , and subsequently the energy, in a self-consistent procedure.

*Interactions.* We focus on the neutron dripline nucleus,  $^{26}\text{O}$ , with the dominating configuration of two neutrons around a  $^{24}\text{O}$  core. The choice of mean-field approximation requires a corresponding effective interaction. For the nucleon-nucleon interactions, we choose the popular Skyrme form [21] with SLy4 parameters [27]. The three-body interaction in Eq. (3) is implemented as a density-dependent two-body interaction.

The Skyrme interaction is of zero range and therefore not directly applicable in Hilbert spaces beyond Slater determinants. The necessary renormalization is possible but requires additional investigations. Instead, we use the finite-range nucleon-nucleon interaction in vacuum for  $V_{A+1,A+2}$  in Eq. (4) [28]. This choice is almost indistinguishable from the result of using a finite-range Gogny-interaction [29] for the mean-field calculation, but in that case the self-consistency would be complete. We leave a more consistent adjustment to future refinements, because this interaction has very little influence on the small-distance structures, while more importantly the large-distance asymptotic properties are correct [28].

The phenomenological density dependence of the Skyrme interaction parametrizes all otherwise omitted influences, e.g., three-body effective forces. These effects are all accounted for by the two-body terms in Eqs. (3) and (4) except for  $\sum_i^A V_{i,A+1,A+2}$ . Again we leave a more consistent derivation to future studies, because this term has very small structure influence, but it is necessary if fine-tuning of the global Skyrme energy is needed. We replace this term by  $V_{c,A+1,A+2} = S_0 \exp(-\rho^2/\rho_0^2)$ , where the hyperradius  $\rho$  is defined as

$$\begin{aligned} (m_n + m_c)\rho^2 = & m_c[(\mathbf{r}_{v_1} - \mathbf{R}_c)^2 + (\mathbf{r}_{v_2} - \mathbf{R}_c)^2] \\ & + m_n(\mathbf{r}_{v_1} - \mathbf{r}_{v_2})^2, \end{aligned} \quad (9)$$

where  $m_n$ ,  $m_c$ , and  $\mathbf{R}_c$  are neutron mass, core mass, and core center-of-mass coordinate, respectively. The range and strength parameters are  $\rho_0 = 6$  fm and  $S_0 = -6.45$  MeV. The Skyrme interactions lead to density-dependent effective masses, which also appear in the coupled Eqs. (8). This is a new feature in three-body equations and in few-body physics in general.

The space allowed for the valence nucleons is only limited by the presence of the identical core nucleons. In the three-body calculation, these core-occupied Pauli forbidden states are removed either by excluding the corresponding lowest adiabatic potentials or by constructing phase equivalent potentials with less bound states [30]. The voluminous and tedious but straightforward derivation along with the subtleties and the space-requiring detailed formulas will be discussed in forthcoming publications.

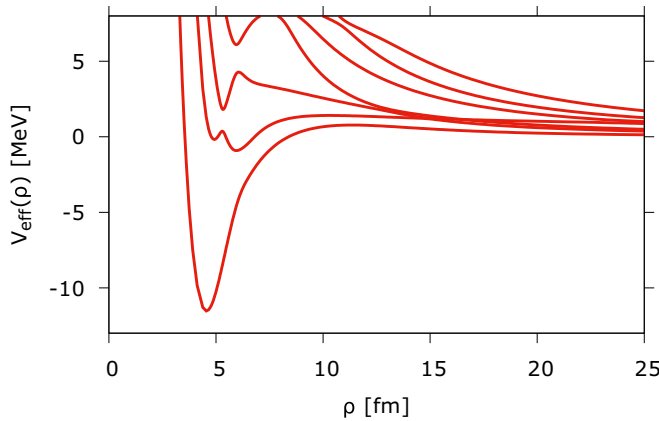


FIG. 1. The lowest adiabatic potentials for the SLy4 interaction, after removal of the Pauli forbidden states. The hyper-radius,  $\rho$ , is normalized with the neutron mass [20].

Meaningful combination and parallel treatment of core and valence spaces require careful selection and perhaps adjustments of the interactions. Our choices are consistent but two less important links between the interactions still need to be fine-tuned. Achieving rigorous consistency is probably difficult in general and the most obvious first application is on small- to large-distance dependence of two-nucleon correlations around a finite nucleus.

*Three-body energies.* With these interactions, we find from Eq. (7) the self-consistent variational solution where the core particles are affected by the valence nucleons and vice versa. We use the hyperspherical adiabatic expansion method [20] for the three-body part where the basic ingredients are the adiabatic potentials displayed in Fig. 1. The lowest potential is attractive at small distances with a wide barrier of height 0.8 MeV. The higher lying potentials are mostly repulsive with features of avoided crossings.

The three-body energy and wave function are found by solving the set of coupled radial equations corresponding to these potentials [20]. The energy,  $E(^{26}\text{O}) = -172.490$  MeV, is obtained for a wave function of the form in Eq. (5), which is 62 keV lower than obtained when the wave function is a pure Slater determinant,  $E_{\text{HF}}(^{26}\text{O}) = -172.428$  MeV. Both these energies are higher than the energy,  $E_{\text{HF}}(^{24}\text{O}) = -172.508$  MeV, obtained by moving the two neutrons infinitely far away, but maintaining the wave function in Eq. (5). Thus, the two-neutron energy is 18 keV in this picture. The influence of the two neutrons on the  $^{24}\text{O}$  core is measured by its distortion energy, which is 285 keV above  $E_{\text{HF}}(^{24}\text{O})$ , within the ground state of  $^{26}\text{O}$ . Therefore, the two neutrons are bound by 267 keV with respect to the distorted  $^{24}\text{O}$  nucleus.

These numbers are compared in Fig. 2, where we notice that our method qualitatively has the correct properties. The  $^{24}\text{O}$  nucleus is excited from its ground state by the presence of the two neutrons. The Hartree-Fock energy of  $^{26}\text{O}$  is higher than  $E(^{26}\text{O})$ , which is reassuring since we should provide an improvement of the pure mean-field calculation. Apparently we have consistently extended both interactions and Hilbert space beyond Slater determinants. Thus, the detailed structure of the wave function is an essential improvement in our model.

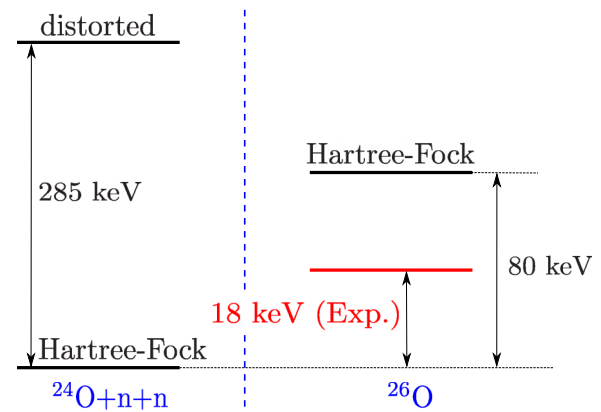


FIG. 2. The distortion energy of  $^{24}\text{O}$  (left) within the  $^{26}\text{O}$  system, and the ground-state energies of  $^{26}\text{O}$  (right) for the Hartree-Fock approximation and the present method. The zero point is the energy of  $^{24}\text{O}$  in the Hartree-Fock ground state.

*Three-body structure.* The probability distribution is shown in Fig. 3 as a function of neutron-neutron distance, and core to neutron-neutron center of mass distance. Two sharp peaks are seen corresponding to a distance between the neutrons and their center of mass and the core of about (6, 2) fm and (3, 3) fm, respectively. These are approximately linear and equal-sided triangular configurations, as shown schematically in Fig. 3. A much fainter peak at distances (4, 1.8) fm is also seen, temptingly interpreted as a dineutron signature. In Ref. [31], the same triple peak structure is obtained using phenomenological interactions, but the dineutron configuration is concluded to be the dominating structure.

To compare properly, we repeated the calculation using the neutron-core potential given in Ref. [31] and found very similar peak structures as in Fig. 3. We find that the dineutron configuration in Ref. [31] is much smaller than, but separated from, the other two peaks. The differences from us are due to different adjustments of neutron-core Woods-Saxon potential

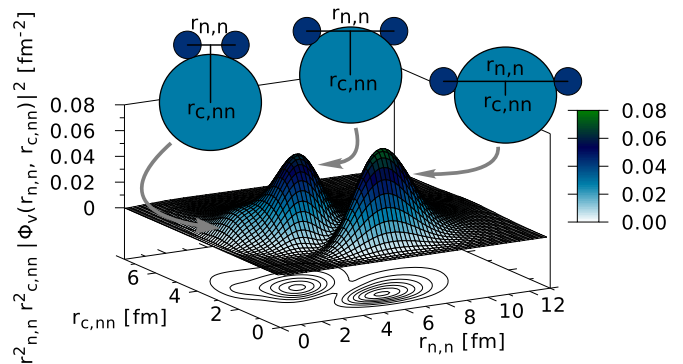


FIG. 3. The probability distribution of the two valence neutrons in  $^{26}\text{O}$  calculated using the Skyrme SLy4 interaction [27] as a function of neutron-neutron distance,  $r_{n,n}$ , and core to neutron-neutron center of mass distance,  $r_{c,nn}$ . The insets are a schematic illustration of the configuration at the peaks.

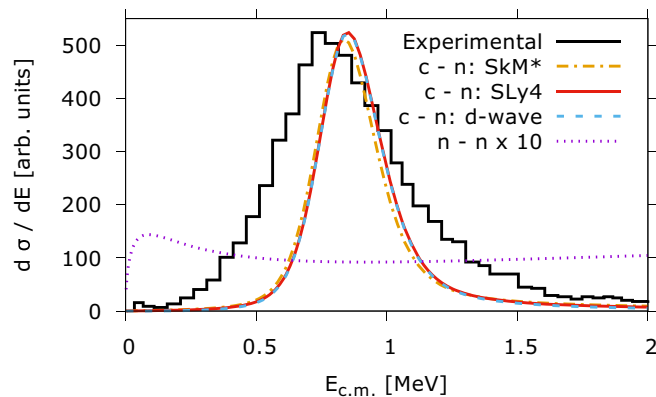


FIG. 4. The invariant mass spectra of core neutron for the SkM\* (dash-dotted, orange) and SLy4 (solid, red) Skyrme parameters. The SLy4 core-neutron  $d$ -wave contribution (dashed, blue) and neutron-neutron (dotted, purple) invariant mass spectrum is also included. The black step curve is the measurements from Ref. [26].

to give the  $^{25}\text{O}$  properties, and the density-dependent neutron-neutron pair potential to give the  $^{26}\text{O}$  energy with the use of the bare nucleon mass. In particular, the last adjustment differs from our model.

We can also study the structure of the  $^{25}\text{O}$  ground-state resonance through the invariant mass spectra of two of the particles after knockout of the third one [32]. The results are shown in Fig. 4, where we first notice the expected structureless neutron-neutron spectrum. The neutron-core spectrum is more interesting with a peak at 0.85 MeV for the SLy4 [27] Skyrme force, and a peak at 0.83 MeV for the SkM\* [33] Skyrme force, which is only 0.1 MeV higher than the experimentally known  $d_{3/2}$  resonance at 0.749(10) MeV [26].

This is in fact a remarkably good agreement for three reasons. First, this result of the neutron-core resonance energy is obtained without any free parameters, that is without any adjustment, and it is found directly from the same interaction as between the nucleons in the core. This is also in contrast to phenomenological models [31], where this two-body energy is used as input parameter. Second, a pure Hartree-Fock calculation of  $^{26}\text{O}$ , with the SLy4 Skyrme force, yields a  $d_{3/2}$  energy of  $-0.96$  MeV. This is a bound state and far from the experimental value, and as such reveals the inadequacy of the Hartree-Fock approximation. Third, the final state in  $^{25}\text{O}$  is populated in two different reactions in experiment and theory, i.e., by high-energy proton and neutron knockout, respectively. Fourth, the resonance energy is reproduced even with a fairly old and less sophisticated Skyrme force such as the SkM\*. This indicates that even a rudimentary core description is enough to yield a core-neutron interaction sufficient to describe the full three-body system in great detail.

The calculated width does not include effects of the unavailable experimental resolution and therefore understandably smaller than the observed value. The neutron-core spectrum is almost indistinguishable from the  $d$ -wave contribution also shown in Fig. 4. This reflects the structure of 90% neutron-core  $d_{3/2}$  wave in the total three-body wave function. The rest is an equal distribution of  $p_{3/2}$ ,  $d_{5/2}$ , and  $f_{7/2}$  waves.

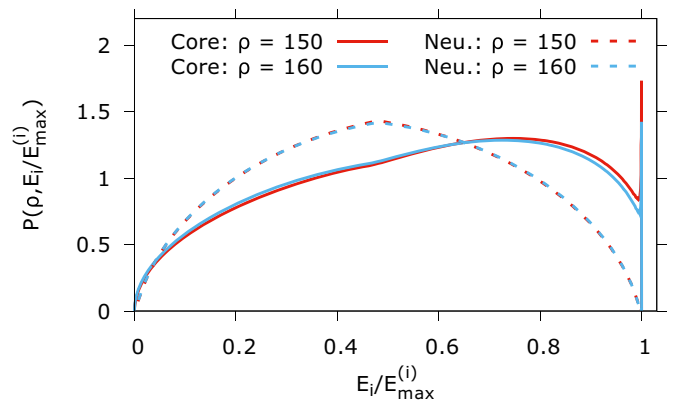


FIG. 5. Single-particle energy distributions after decay of the ground-state resonance [35,36]. Here  $E_i$  is core (solid) or neutron (dashed) energy, and  $E_{\max}^{(i)}$  is the maximum energy available for particle  $i$ , while red (gray) and blue (light-gray) correspond to  $\rho = 150$  and  $\rho = 160$  fm, respectively. The peak for the core energy is due to numerical inaccuracies.

*Lifetime and decay properties.* As already mentioned, a central aspect of the present method is how the presence of the valence nucleons affects the core. This is reflected in distortion of the core wave function and therefore also in the energy. By going from small to large values of hyper-radius,  $\rho$ , the core should change from a distorted structure to the free solution. However, currently only the average effect is included and the core structure is maintained for all distances. This lack of a gradual relaxation means that while the bulk part of the calculated potential in Fig. 1 is correct, the large-distance asymptotic value of the potential is too high, in this case by 285 keV. However, by extending the adiabatic approach and solving the coupled expressions from Eq. (8) for each step in  $\rho$ , a smooth transition could be obtained. We leave this more elaborate procedure for future improvements, because this would only marginally change any of the observables except possibly the width.

This width of the  $^{26}\text{O}$  ground-state resonance can still be fairly well estimated in the present implementation as the oscillator-approximated knocking rate multiplied by the WKB tunneling probability through the modified barrier in the lowest adiabatic potential [34]. First, we shift the full adiabatic potential by 285 keV. This leads to an outer turning point of 66.3 fm and a lifetime of  $10^{-16}$  s. Instead, when only lowering the potential by 285 keV in the tail outside 66.3 fm, the well-defined outer turning point at the energy of  $18 - 285 = -267$  keV leads to a lifetime of about  $10^{-15}$  s. Experimentally, the half-life is found to be between  $10^{-17}$  s and  $10^{-15}$  s [26], and we conclude that even when employing a very crude transition mechanism this exponentially sensitive observable is predicted remarkably well by the model.

The resonance is decaying into two neutrons and the core. Following Refs. [35,36], the single-particle energy distributions after decay are obtained in coordinate space from the stable spatial distribution of the particles for large values of  $\rho$ , where the hyperangles in coordinate and momentum space coincide. The results are shown in Fig. 5 for two  $\rho$  values, 150 and 160 fm, to show convergence. The extremes, where one

particle takes either maximum or zero energy, leaves either zero or maximum energy in the relative motion between the other two particles.

We then see in Fig. 5 that the core energy is weighted toward its maximum with a corresponding decreasing fraction left for the relative motion of the neutrons (solid curves). Each neutron has largest probability for appearing with half of its maximum energy, again implying that the other half is in relative neutron-core motion (dashed curves). This shows that the decay mechanism is direct population of the continuum, consistent with the fact that the  $d_{3/2}$  resonance in  $^{25}\text{O}$  is too high in energy to be even virtually populated during the decay.

*Summary.* The present study provides a consistent, flexible, and computationally efficient approach to including the intricacies of few-body formalisms into a many-body context. The model is practical and efficient as demonstrated in the application on the challenging nuclear neutron dripline nucleus,  $^{26}\text{O}$ . The data of both  $^{25}\text{O}$  and  $^{26}\text{O}$  are reproduced with fewer parameters than found in dedicated phenomenological models. Furthermore, the exponentially sensitive lifetime is

obtained within measured uncertainties. This is particularly remarkable considering the simple self-consistent Skyrme-Hartree-Fock calculation for the core. In the future, this could be replaced by more sophisticated methods.

The novel features of the quantum mechanical model are that few- and many-body properties respectively at large and small distances are self-consistently connected. The model is applicable to both bound and continuum states and addresses challenges in open quantum systems. In addition, the efficiency and flexibility of this method opens up the possibility of examining heavy, many-particle systems in full detail without incurring insurmountable computational difficulties. The universal character of halos and Efimov states suggests applications in other subfields of physics.

*Acknowledgments.* This work was funded by the Danish Council for Independent Research DFF Natural Science and the DFF Sapere Aude program. This work has been partially supported by the Spanish Ministerio de Economía y Competitividad under Project FIS2014-51971-P. We acknowledge many fruitful discussions with Karsten Riisager.

- 
- [1] M. Bender, P.-H. Heenen, and P.-G. Reinhard, *Rev. Mod. Phys.* **75**, 121 (2003).
- [2] T. Nikšić, D. Vretenar, and P. Ring, *Prog. Part. Nucl. Phys.* **66**, 519 (2011).
- [3] J. Dobaczewski, *J. Phys. G: Nucl. Part. Phys.* **43**, 04LT01 (2016).
- [4] E. Epelbaum, H.-W. Hammer, and U.-G. Meissner, *Rev. Mod. Phys.* **81**, 1773 (2009).
- [5] J. Carlson, S. Gandolfi, F. Pederiva, S. C. Pieper, R. Schiavilla, K. E. Schmidt, and R. B. Wiringa, *Rev. Mod. Phys.* **87**, 1067 (2015).
- [6] H. Hergert, S. K. Bogner, T. D. Morris, A. Schwenk, and K. Tsukiyama, *Phys. Rep.* **621**, 165 (2016).
- [7] K. Hebeler, J. D. Holt, J. Menendez, and A. Schwenk, *Annu. Rev. Nucl. Part. Sci.* **65**, 457 (2015).
- [8] A. Ono, H. Horiuchi, T. Maruyama, and A. Ohnishi, *Prog. Theor. Phys.* **87**, 1185 (1992).
- [9] H. Feldmeier and J. Schnack, *Prog. Part. Nucl. Phys.* **39**, 393 (1997).
- [10] Y. C. Tang and M. LeMere, *Phys. Rep.* **47**, 167 (1978).
- [11] I. Rotter and J. P. Bird, *Rep. Prog. Phys.* **78**, 114001 (2015).
- [12] B. R. Barrett, P. Navrátil, and J. P. Vary, *Prog. Part. Nucl. Phys.* **69**, 131 (2013).
- [13] W. Leidemann and G. Orlandini, *Prog. Part. Nucl. Phys.* **68**, 158 (2013).
- [14] S. Liebig, U.-G. Meissner, and A. Nogga, *Eur. Phys. J. A* **52**, 103 (2016).
- [15] G. Hagen, M. Hjorth-Jensen, G. R. Jansen, and T. Papenbrock, *Phys. Scr.* **91**, 063006 (2016).
- [16] C. Romero-Redondo, S. Quaglioni, P. Navratil, and G. Hupin, *Phys. Rev. Lett.* **117**, 222501 (2016).
- [17] A. Calci, P. Navratil, R. Roth, J. Dohet-Eraly, S. Quaglioni, and G. Hupin, *Phys. Rev. Lett.* **117**, 242501 (2016).
- [18] T. Frederico, A. Delfino, L. Tomio, and M. T. Yamashita, *Prog. Part. Nucl. Phys.* **67**, 939 (2012).
- [19] E. Braaten and H.-W. Hammer, *Phys. Rep.* **428**, 259 (2006).
- [20] E. Nielsen, D. V. Fedorov, A. S. Jensen, and E. Garrido, *Phys. Rep.* **347**, 373 (2001).
- [21] D. Vautherin and D. M. Brink, *Phys. Rev. C* **5**, 626 (1972).
- [22] B. A. Brown and W. A. Richter, *Phys. Rev. C* **72**, 057301 (2005).
- [23] C. R. Hoffman, T. Baumann, D. Bazin, J. Brown *et al.*, *Phys. Lett. B* **672**, 17 (2009).
- [24] Z. Kohley, T. Baumann, D. Bazin, G. Christian *et al.*, *Phys. Rev. Lett.* **110**, 152501 (2013).
- [25] C. Caesar, J. Simonis, T. Adachi, Y. Aksyutina *et al.*, *Phys. Rev. C* **88**, 034313 (2013).
- [26] Y. Kondo, T. Nakamura, R. Tanaka, R. Minakata *et al.*, *Phys. Rev. Lett.* **116**, 102503 (2016).
- [27] E. Chabanat, P. Bonche, P. Haensel, J. Meyer, and F. Schaeffer, *Nucl. Phys. A* **635**, 231 (1998).
- [28] E. Garrido and E. Moya de Guerra, *Nucl. Phys. A* **650**, 387 (1999).
- [29] J. Decharge and D. Gogny, *Phys. Rev. C* **21**, 1568 (1980).
- [30] E. Garrido, D. V. Fedorov, and A. S. Jensen, *Nucl. Phys. A* **650**, 247 (1999).
- [31] K. Hagino and H. Sagawa, *Phys. Rev. C* **93**, 034330 (2016).
- [32] M. Zinser, F. Humbert, T. Nilsson, W. Schwab *et al.*, *Nucl. Phys. A* **619**, 151 (1997).
- [33] J. Bartel, P. Quentin, M. Brack, C. Guet, and H. B. Hkansson, *Nucl. Phys. A* **386**, 79 (1982).
- [34] E. Garrido, D. V. Fedorov, and A. S. Jensen, *Nucl. Phys. A* **733**, 85 (2004).
- [35] E. Garrido, D. V. Fedorov, H. O. U. Fynbo, and A. S. Jensen, *Nucl. Phys. A* **781**, 387 (2007).
- [36] H. O. U. Fynbo, R. Álvarez-Rodríguez, A. S. Jensen, O. S. Kirsebom, D. V. Fedorov, and E. Garrido, *Phys. Rev. C* **79**, 054009 (2009).